PHILOSOPHICAL TRANSACTIONS OF THE ROYAL SOCIETY B BIOLOGICAL SCIENCES

The Croonian Lecture 2000. Nicotinic acetylcholine receptor and the structural basis of fast synaptic transmission,Lecture delivered 5 October 2000 at University College London

Nigel Unwin

Phil. Trans. R. Soc. Lond. B 2000 **355**, 1813-1829
doi: 10.1098/rstb.2000.0737

THE ROYAL SOCIETY

doi 10.1098/rstb.2000.0737

The Croonian Lecture 2000. Nicotinic acetylcholine receptor and the structural basis of fast synaptic transmission

Lecture delivered 5 October 2000 at University College London

Nigel Unwin

Medical Research Council Laboratory of Molecular Biology, Hills Road, Cambridge CB2 2QH, UK

Communication in the nervous system takes place at chemical and electrical synapses, where neurotransmitter-gated ion channels, such as the nicotinic acetylcholine (ACh) receptor, and gap junction channels control propagation of electrical signals from one cell to the next. Newly developed electron crystallographic methods have revealed the structures of these channels trapped in open as well as closed states, suggesting how they work. The ACh receptor has large vestibules extending from the membrane which shape the ACh-binding pockets and facilitate selective transport of cations across a narrow membrane-spanning pore. When ACh enters the pockets it triggers a concerted conformational change that opens the pore by destabilizing a gate in the middle of the membrane made by a ring of pore-lining α-helical segments. The alternative 'open' configuration of pore-lining segments reshapes the lumen and creates new surfaces, allowing the ions to pass through. The gap junction channel uses a similar structural mechanism, involving coordinated rearrangements of α-helical segments in the plane of the membrane, to open its pore.

Keywords: acetylcholine receptor; gap junction; synapse; electron microscopy

1. INTRODUCTION

Almost 40 years ago Sir Bernard Katz delivered a Croonian lecture on a topic related to my own. The title of his talk was 'The transmission of impulses from nerve to muscle, and the subcellular unit of synaptic action' (Katz 1962). He described a series of electrophysiological experiments in which he had dissected the process of rapid chemical communication between nerve and muscle into a number of separable steps. That is reduction of the resting potential of the nerve terminal membrane; release in discrete 'quanta' of the neurotransmitter acetylcholine (ACh); diffusion of ACh across the synaptic cleft; binding of ACh to receptors in the postsynaptic membrane of the muscle cell; and an increase in cation permeability of the postsynaptic membrane and its resultant depolarization, initiating the signal for the muscle to contract. Sir Bernard ended his lecture by emphasizing the need for a molecular visualization of the events; referring to the postsynaptic membrane: '...What is the chemical constitution of the cell surface; What are the molecular properties which determine its selectivity for ions, and how are these properties altered when a substance like ACh combines with some of the membrane molecules?'

A much more detailed understanding of chemical synaptic transmission has come about since that time as a result of major advances in electrophysiological and microscopical techniques, and the remarkable progress in molecular biology. One key development in terms of describing the initial steps was made by John Heuser and his collaborators when they succeeded in freezing nerve terminals at the frog neuromuscular junction a precise interval after a stimulus by slamming them into a block of metal cooled by liquid helium. The freeze-fracture images showed pits in the presynaptic membrane in numbers which were proportional to the number of quanta released (Heuser *et al.* 1979). These results thereby firmly linked the process of vesicular fusion (exocytosis) and quantal neurotransmitter release.

Neurotransmitter release and the cycling of synaptic vesicles continues to be a topic of intense research (for recent reviews, see Fernandez-Chacon & Sudhof 1999; Marsh & McMahon 1999), and it has even become possible to image single synaptic vesicles as they move to the membrane and fuse there (Zenisek *et al.* 2000). However, my main purpose in this paper is to discuss the final step in synaptic transmission, involving the rapid excitatory or inhibitory events occurring at the postsynaptic membrane, rather than action on the presynaptic side. Increased knowledge about neurotransmitter-gated channels, selective for positive or negative ions, has greatly extended our concept of the postsynaptic membrane of 40 years ago. We now know, for example, that there are two main groups of such ion channels, based on amino-acid sequence: those of the ACh receptor family, which include the $GABA_A$ (γ-aminobutyric acid type A), glycine, $5\text{-}HT_3$ (5-hydroxytryptamine type 3) and neuronal ACh receptors; and those of the glutamate receptor family: the AMPA (α-amino-3-hydroxy-5-methyl-4-isoxazoleproprionate), kainate and NMDA (*N*-methyl-D-aspartate) receptors.

Also important are gap junction channels, the mediators of fast electrical synaptic transmission between connected pairs of nerve cells. There is an enormous diversity of these synaptic channels, arising not just from the different members of different families, but also from the wide range of subunit types and distinct subunit combinations used by the cell.

In the tradition of a Croonian lecture, I will stress areas of personal interest and involvement leading to our present level of understanding of structure and mechanism. Most of the experiments I will refer to have been conducted on the postsynaptic membranes of electrocytes from the *Torpedo* electric ray. Electrocytes are modified muscle cells, and their postsynaptic membranes resemble those of the neuromuscular junction, organizing into a series of folds opposite the active zones where ACh is released (Whittaker 1992). ACh receptor ion channels and the receptor-clustering protein, rapsyn, are present in high concentrations at the crests of these folds (Sealock *et al.* 1984). Although the chemical nerve–nerve synapses of the central and peripheral nervous systems use different sets of postsynaptic proteins, they make use of the same, or similar, principles to achieve fast synaptic transmission. The electrocyte membranes of the *Torpedo* ray, like those of the neuromuscular junction, provide in many respects an ideal system for elucidating these principles.

2. DEVELOPMENT OF NEW IMAGING METHODS

The freeze-fracture studies on the frog neuromuscular junction were landmark experiments because they were the first to visualize clearly synaptic events occurring on a millisecond time-scale. With the freeze-fracture method, however, freezing is used at the beginning of the specimen preparation process, while at the end it is always just a surface replica that is observed in the electron microscope. Direct examination of the specimen itself was needed to learn about intact three-dimensional (3D) structure. The first successful attempts at recording images from frozen biological objects were by Taylor & Glaeser (1976). They found that the ice-embedded specimens were stable in the microscope vacuum when held in a cold stage at temperatures below $-100\,^{\circ}\mathrm{C}$. But the technology—now called cryomicroscopy—only became established some time later, as a result of some simplifying improvements and the commercial manufacture of cold stages. Especially important were the procedures of blotting the sample to obtain a thin aqueous film on the microscope grid, and then plunging the grid rapidly into liquid nitrogen-cooled ethane to create amorphous, rather than crystalline ice (Lepault *et al.* 1983; Dubochet *et al.* 1988).

To combine the needs both to image the specimen directly and to capture synaptic events on the millisecond time-scale John Berriman and I modified the cryo-plunger into a spray-freezing device (Berriman & Unwin 1994). An atomizer spray gun is activated the moment the microscope grid, held in the plunger, is released, so that a burst of spray droplets, containing ACh and ferritin marker particles, impinge on the grid just (*ca.* 5 ms) before it hits the ethane surface. In this way, the ACh in the droplets can be mixed with the film containing postsynaptic membranes over an interval long enough to open the channels, while ensuring that a negligible fraction of them convert to a desensitized form. Rapid dilution of the impacted spray droplets occurs by surface spreading and diffusion, but the final concentration of ACh in the vicinity of the specimen can be estimated from the image by the number of ferritin particles present. The ethane immersion achieves nearly instantaneous trapping of the reaction because the freezing rate (*ca.* $10^6\,^{\circ}\mathrm{C\,s^{-1}}$) is very fast.

3. THREE-DIMENSIONAL STRUCTURES FROM IMAGES

In addition to the requirements of directly viewing the specimen, and of capturing transient structural changes, methods had to be developed for extracting 3D information from the electron micrographs. The contrast generated by electrons interacting with organic matter is extremely weak. Furthermore, biological molecules are highly sensitive to electron damage, and fall apart at doses far smaller than those used in routine observations of stained samples. If the images are recorded with a dose small enough to avoid damage, they will be too noisy to show fine structure with clear definition.

It had long been recognized that it should be possible to surmount this statistical deficiency by averaging the details contained in large numbers of identical molecules (McLachlan 1958). Genuine features common to each molecule would be reinforced by the averaging, while the fluctuations associated with electron noise (which differ from one molecule to the next) would be smeared out. Richard Henderson and I made use of this principle in our studies of the crystalline, bacteriorhodopsin-containing purple membranes (Unwin & Henderson 1975), using the water-substituting medium, glucose, to retain the native structure of the membrane in the microscope vacuum. Although micrographs of the glucose-embedded membranes recorded with an appropriate low electron dose were too noisy for the individual bacteriorhodopsin molecules to be distinguished by eye, the averaging of large numbers of identical molecules enabled us to reveal the arrangement of the seven α-helical segments crossing the lipid bilayer.

We accomplished the averaging by densitometering the micrographs to convert them into arrays of optical densities, and analysing the arrays by the computational Fourier method developed for reconstructing 3D structures from negatively stained macromolecules (DeRosier & Klug 1968). The Fourier transform of the image of a crystal separates the signal (which is at discrete points on a lattice) from the noise (which lies in-between these points) and thereby achieves a result equivalent to that obtainable by superimposing the molecules one at a time and averaging them in 'real space'. However, the Fourier approach, in which the object is decomposed into its sine wave components, each having a distinct amplitude and phase, is more adaptable to rapid computation and quantitative evaluation, and can more readily be extended to the analysis of 3D structures.

How is a 3D structure determined from a two-dimensional (2D) crystal, such as purple membrane, when an image displays only a single view—a projection

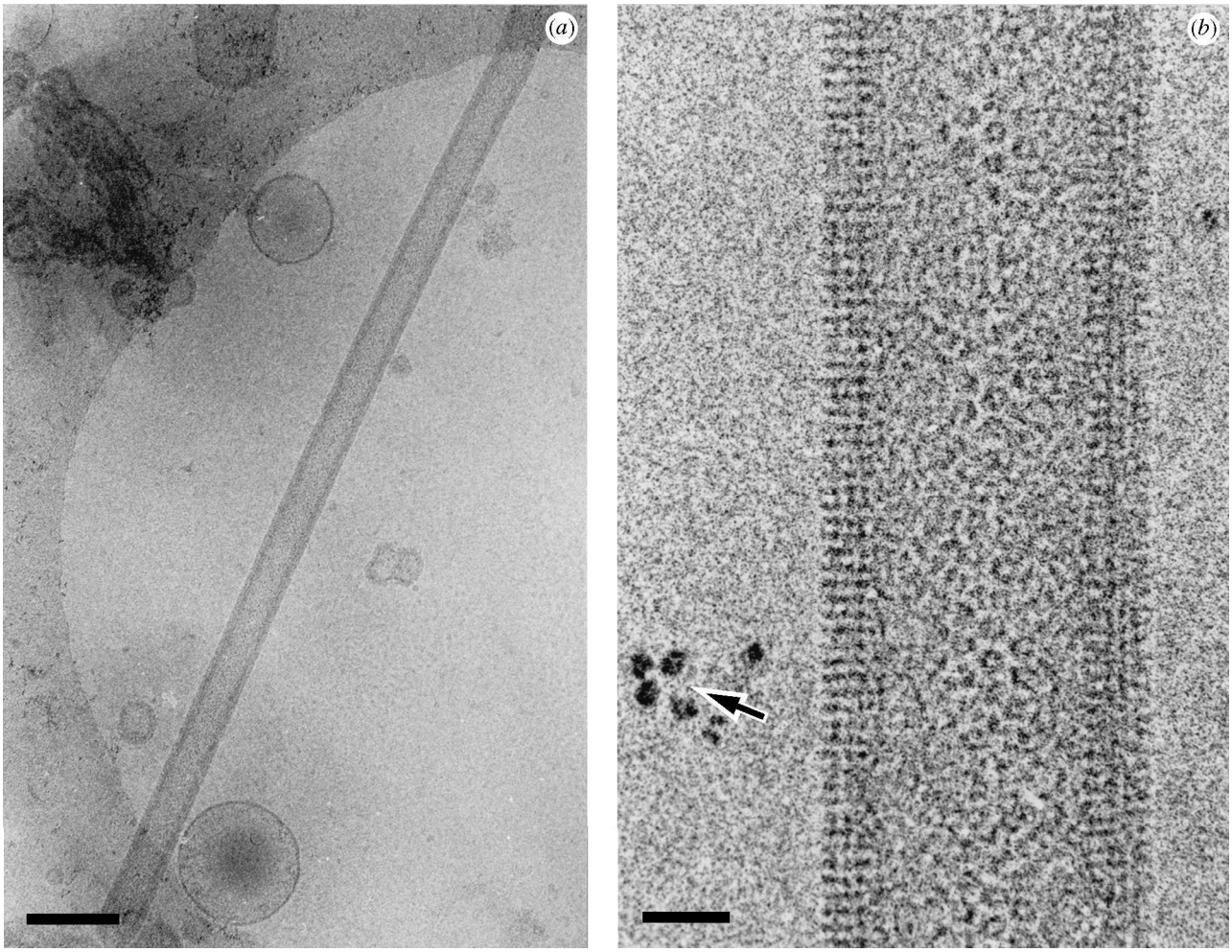

Figure 1. ACh receptor tubes are imaged in thin films of amorphous ice over holes in the carbon support film. (*a*) Low magnification image, (*b*) high magnification image, showing receptors face-on near the middle of the tube, and side-on at the edges. To obtain receptors in the open-channel form, ACh-containing droplets are sprayed onto the microscope grid containing the tubes *ca*. 5 ms before the rapid freezing. Ferritin marker particles (arrow), included in the spray solution, identify tubes that have been reacted with ACh. Scale bars, (*a*) 2000 Å and (*b*) 200 Å.

of the densities? The answer is to obtain a number of different views and to combine them, making use of the property that each corresponds to a different central section through the 3D Fourier transform (DeRosier & Klug 1968; Henderson & Unwin 1975). Once this Fourier transform has been sampled by the different central sections at a sufficient number of points to trace accurately the amplitude and phase variations, the structure can be calculated by a 3D Fourier synthesis.

Tubular crystals form the basis of almost all quantitative structural studies of postsynaptic membranes. Tubes differ most obviously from 2D crystals in that their lattice, instead of being planar, makes a continuous network around the surface of a cylinder. For structure analysis, they are most usefully thought of as one-dimensional crystals (giving rise to regularly spaced layer-lines, rather than spots, in their Fourier transforms), and as objects built up from helical density waves (Klug *et al.* 1958; Moody 1990). Thus the layer-lines each give information about a particular set of helical waves, the number around the circumference of which is a property of the helical symmetry present. The measured amplitudes and phases along the layer-lines allow the azimuthal variation in strength and relative positions of these waves to be calculated, and hence provide all that is required to derive the average 3D structure (DeRosier & Moore 1970). This property of a tubular crystal, arising from its helical construction, makes it unnecessary to carry out tilting experiments, as needed to acquire different views with a 2D crystal. But the principle of averaging over many identical units to achieve a high signal-to-noise ratio is the same.

4. PROPERTIES OF ACh RECEPTOR TUBES

A special feature of the electrocytes is the dense, partially crystalline packing of ACh receptors on their innervated faces. Freeze-fracture photographs show the receptors on the membrane surface to be grouped as dimers, and organized as paired ribbons packed tightly side-by-side (Heuser & Salpeter 1979). Tubes are also composed of tightly packed ribbons of receptor dimers (Brisson & Unwin 1984), and grow naturally from the isolated electrocyte membranes (Kubalek *et al.* 1987), retaining a similar curvature as the crests of the junctional folds. Clearly there is a close structural

correspondence between the tubes, which are simply elongated protein–lipid vesicles, and the receptor-rich membrane as it exists *in vivo*.

The ACh receptor, forming the surface lattice of the tube, is a model neurotransmitter-gated ion channel that has been explored intensively over the last 25 years by all kinds of techniques (Hille 1992). It is a large (*ca.* 290 kDa) glycoprotein composed of a ring of five subunits which together delineate a gated cation-selective pathway across the membrane. There are two ACh-binding (α) subunits, having identical amino-acid sequences, and three others (β, γ and δ) having sequences homologous to the αs (42, 35 and 36% identity to α, respectively; Popot & Changeux 1984). Each subunit has a large extracellular N-terminal domain, four predicted transmembrane regions (M1–M4), and an extended cytoplasmic M3–M4 loop. In evolutionary terms, the β-subunit diverged first from the α-subunit, along a separate path from the γ/δ lineage (Kubo *et al.* 1985), suggesting it has a distinct functional role. The γ- and δ-subunits influence most strongly the ACh-binding properties of the α-subunits. The δ-subunit of the *Torpedo* receptor has near its C-terminus a cysteine residue, which forms intermolecular δ–δ disulphide bridges (Chang & Bock 1977; McCrea *et al.* 1987). This covalent linkage accounts for the observed pairing of the *Torpedo* receptors, since the they disperse rapidly on exposure to reducing agents (Brisson & Unwin 1984).

Early microscopical studies of the tubes were limited in resolution to *ca.* 30 Å, because of the flattening caused by their interaction with the carbon support film (Kistler & Stroud 1981; Brisson & Unwin 1984, 1985; Mitra *et al.* 1989; Kubalek *et al.* 1987). However, Chikashi Toyoshima and I found that the tubes retained their cylindrical cross-section in regions of amorphous ice where they were totally surrounded by water, i.e. over holes in the carbon support film (figure 1). Images of tubes from such regions, when analysed by the helical method, yielded 3D maps at 17 Å resolution (Toyoshima & Unwin 1990). The improved maps showed the protein subunits to be long rods arranged around a pseudo-five-fold axis in an orientation approximately normal to the membrane plane. The ion-conducting pathway, delineated by the symmetry axis, consisted of a narrow pore across the lipid bilayer bounded by 20–25 Å diameter vestibules that extended *ca.* 65 Å into the synaptic cleft and *ca.* 20 Å towards the interior of the cell (figure 2). A large centrally located mass at the cytoplasmic end of the receptor was thought to be composed of the 43 kDa receptor-clustering protein, rapsyn, because it was not present in maps calculated from tubes imaged in alkaline pH (Toyoshima & Unwin 1988), a condition known to release this protein (Neubig *et al.* 1979). However, later studies (see §8) revealed that the receptor extends into this central mass. The loss in visibility was therefore presumably due to local disorder induced by the alkaline pH.

5. 9 Å MODEL OF THE ACh RECEPTOR

A major aim of the electron microscopical studies is to see the receptor in atomic detail and so provide a 3D chemical framework for bringing together the extensive

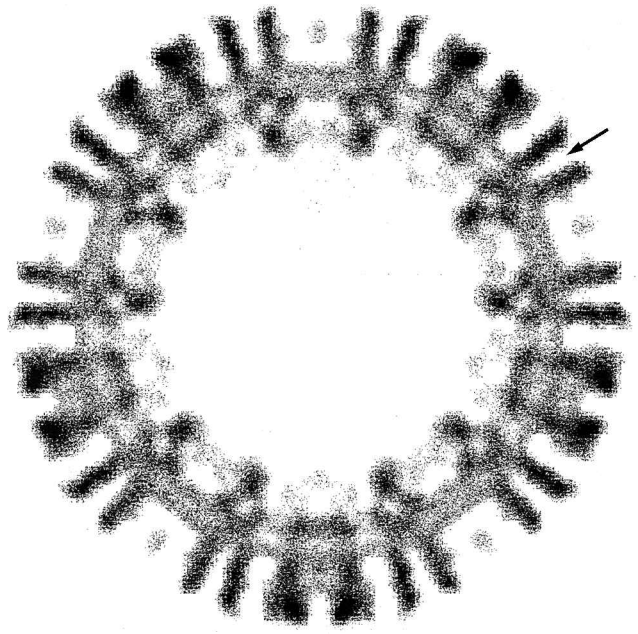

amount of information obtained from other kinds of investigation. But the technology for doing this has not been available and so it has only been feasible to progress towards this goal in steps. Radiation damage is a particular concern in the structure analysis of tubes. A tube typically contains only 1000–3000 regularly arranged receptor molecules—not enough to yield a good signal-to-noise ratio beyond *ca.* 17 Å resolution. To improve on this, more molecules need to be averaged by combining data from different tubes. A resolution of 9 Å was achieved initially using data from 26 tubes (*ca.* 50 000 receptors) (Unwin 1993). In going beyond 9 Å, as I will describe later, not only do many more molecules need to be averaged, but corrections need to be made for small distortions of the tubular lattices (Beroukhim & Unwin 1997), and the images must be of the highest possible electron optical quality. The quality of the image is a critical factor in the structure analysis of tubes, where the more accurate measurement of amplitudes from electron diffraction patterns cannot be done. All recent recording of images have therefore been conducted in Japan, using a 300 kV field emission microscope incorporating an exceptionally stable liquid helium-cooled specimen stage (Fujiyoshi *et al.* 1991; Fujiyoshi 1998).

The 9 Å map revealed several unsuspected features and gave new clues about how the receptor works. In the extracellular portion, *ca.* 30 Å from the membrane surface, the two α-subunits were found to contain internal cavities (figure 3). These cavities were each of about the right size to accommodate an ACh molecule, suggesting that they might be the actual pockets where ACh binds. The binding sites did not appear to be at the α–γ subunit and α–δ subunit interfaces, as was (and still is) the widely held view.

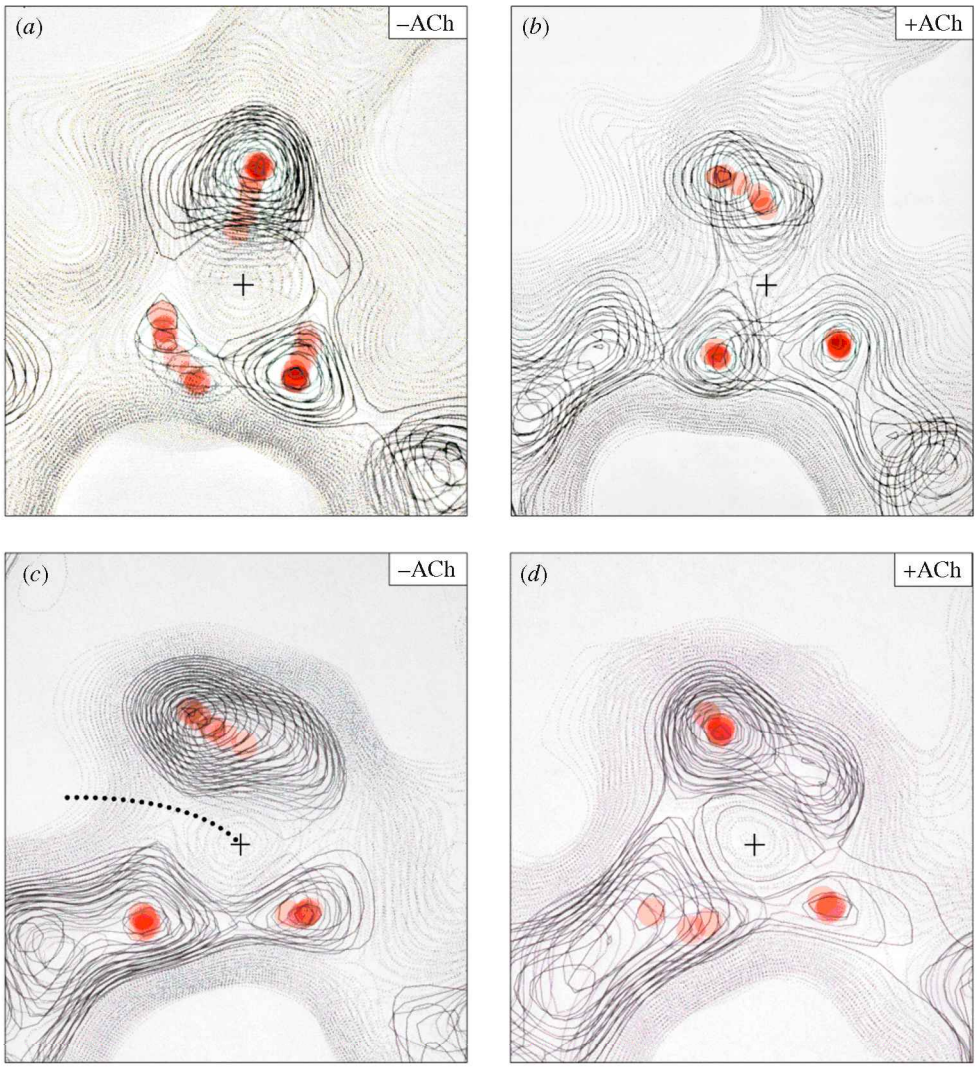

Figure 3. Detail at 9 Å around cavities forming the ACh-binding pockets in the two α-subunits before (−ACh) and after (+ACh) brief exposure to ACh. (*a*,*b*) α_δ-subunits and (*c*,*d*) α_γ-subunits. The three rods of density encircling the α_δ-cavity (pink traces) appear to twist around its centre (+) upon binding of ACh. The three rods of density encircling the α_γ-cavity are already in a configuration close to that of α_δ with ACh bound, and do not change so much upon binding of ACh. The dotted line in α_γ (−ACh) follows a tunnel connecting the cavity to the external surroundings (see also figure 10*b*). The contour maps are 12 Å thick slabs cut through the structure in a plane normal to the receptor axis at a level *ca*. 30 Å from the membrane surface; the extracellular vestibule is located at the bottom of each panel.

Also surprising, in the membrane-spanning portion of each subunit, there was only one (α-helical) rod clearly visible, not four as predicted from hydropathy plots. The single rod visible in each subunit formed the wall lining the pore, and presumably corresponded to the predicted transmembrane α-helix, M2, since several kinds of experiment had converged to indicate that this stretch was exposed to the ions (Hucho *et al.* 1986; Giraudat *et al.* 1986; Imoto *et al.* 1988; Leonard *et al.* 1988). The M2 rod did not form a straight path through the lipid bilayer, but bent near its midpoint, where it was closest to the pore axis (figure 4*a*). On the lipid-facing sides it was flanked by a continuous rim of density, likely to be composed of β-sheet.

A tentative alignment was able to be made between the 3D densities and the amino-acid sequence of M2. This alignment placed the charged groups at the end of M2 symmetrically on either side of the bilayer, and a highly conserved leucine residue (*Torpedo* αLeu251; Unwin 1989) at the level of the bend (figure 4*b*). It was suggested that the gate of the channel might be made by the leucine side-chains projecting into the pore from the bends and associating side-to-side to create a tight hydrophobic barrier that would prevent passage of the hydrated ions.

Mutagenesis combined with electrophysiological study of function has been a valuable approach for identifying the likely roles played by individual M2 side-chains in affecting ion permeation. Several such experiments have highlighted the uniqueness of the conserved leucine residue in relation to the gating mechanism. For example, replacement of successive leucines in the ACh receptor by serines (Labarca *et al.* 1995) or by threonines (Filatov & White 1995) increased markedly, by uniform increments, the opening sensitivity of the channel. Replacement of the leucine with threonine in the $GABA_A$ receptor, an ion channel in the same family, allowed ion conduction in the absence of agonist, suggesting an almost total shift in equilibrium towards the open-channel form (Tierney *et al.*

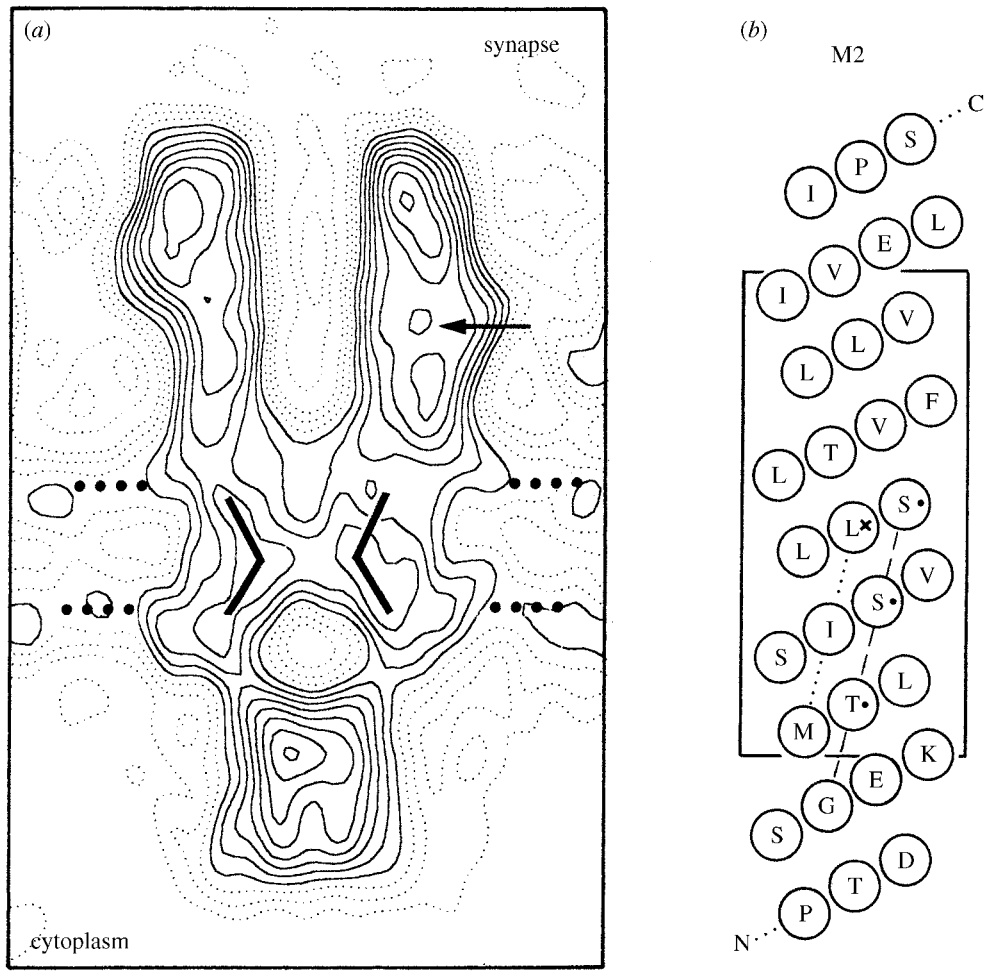

Figure 4. Interpretation of the closed-channel structure at 9 Å. (*a*) Channel in profile with positions of the pore-lining M2 rods, level of the ACh-binding pockets (arrow) and estimated limits of the lipid bilayer (dotted lines, 30 Å apart) indicated. (*b*) Helical net plot of the amino-acid sequence around the segment M2 (*Torpedo* α-subunit); the cross denotes the conserved leucine residue, L251, which may form the gate of the channel; the dots denote other residues that have been shown to affect the binding affinity of an open channel blocker (Leonard *et al*. 1988; Charnet *et al*. 1990), and ion flow through the open pore (Villarroel *et al*. 1991). Adapted from Unwin (1993).

1996). However, the effect of a mutation in the functional region of a simple protein cannot be predicted even when the atomic structure is known (e.g. Craik *et al*. 1985). Thus a definitive interpretation of the role of the leucine is not possible from this kind of experimental approach.

6. DISTINCT CONFORMATIONS OF THE α-SUBUNITS

One interesting observation made at this stage, but not published, was that the two α-subunits looked different, despite their amino-acid sequences being the same. The α_δ-cavity was more circular in cross-section, and the three rods of density shaping the cavities were not equivalent in the two subunits (figure 3). Were their different appearances genuine ones brought about because these subunits might be unequally distorted by their different sets of interactions with neighbouring subunits? Or were their differences due to systematic errors associated with the helical method of structure determination (which had not previously been applied to such high resolution)?

The differences were indeed genuine properties of the receptor, as was shown by an alternative structural approach. Occasionally it is possible to obtain 'giant' ACh receptor tubes from the vesicle preparations. Such tubes are 2000–3000 Å across, and can be flattened uniformly on the microscope grid, making them amenable to analysis as (overlapping) 2D crystals. The two independently determined structures, obtained from cylinders on the one hand and planar arrays on the other, showed the same differences between the α-subunits, confirming unequivocally that these subunits do have different conformations in the closed-channel form of the receptor (Unwin 1996).

7. CHANGES UPON ACTIVATION BY ACh

The receptor channels open with remarkable speed and efficiency at the synapse, when triggered by entry of ACh molecules into their binding pockets. They open within about 20 μs of binding and achieve a high probability of opening (*ca*. 0.95) until the ACh has been degraded by acetylcholinesterase or until desensitization takes place (Colquhoun & Sakmann 1985). Desensitization occurs within *ca*. 20 ms in the continued presence of ACh (Matsubara *et al*. 1992). Thus in order to convert the

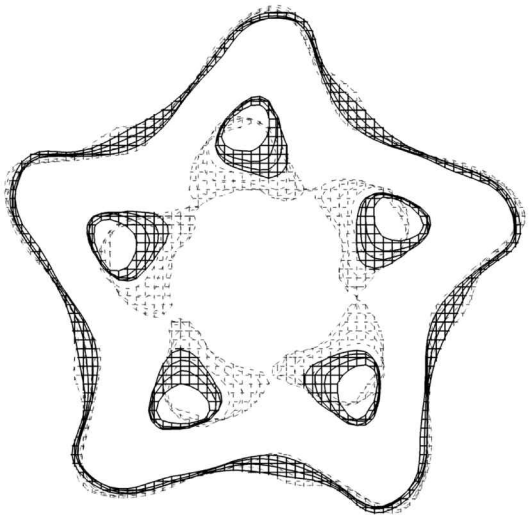

Figure 5. ACh-induced changes at the level of the gate, in the middle of the membrane. The M2 rods are *ca.* 2 Å further from the central axis after (full lines) than before (broken lines) exposure to ACh. In contrast, the outer rim of density does not change significantly (indicated by almost exact superposition of the two contours).

receptor into the open-channel form and retain this form so that its structure can be analysed, extremely brief reaction with ACh is needed, followed by trapping of the structural response.

I described above in § 2 the method devised to achieve and trap the open channel. In brief, a solution of ACh, containing ferritin marker particles, is sprayed onto tubes in a thin aqueous film on the electron microscope grid, and the grid is then plunged rapidly (within 5 ms) into liquid nitrogen-cooled ethane. Since a 3D structure of the receptor can be derived from a single image of a tube, it was possible to investigate systematically the effect of exposure to different concentrations of ACh (which could be estimated from the number of ferritin particles in the image). I found there was a small, but reproducible structural change over concentrations used in the data collection (100 µM–10 mM), as would be expected if there were always a high proportion of open channels under these conditions (Unwin 1995). On the other hand prolonged, desensitizing exposure to ACh gave rise to a much greater and different kind of change.

The transition from the closed to the open channel was analysed by comparing the new map from the sprayed tubes (also at 9 Å resolution, from *ca.* 50 000 molecules) with the old. Most affected was the region around and close to the cavities, i.e. the ACh-binding pockets. The disturbance at this level was complex, involving all five subunits. However, it is useful to focus on the α-subunits, one of which (α_δ figure 3*a*,*b*) was altered a large amount by the interaction with ACh, and the other of which (α_γ; figure 3*c*,*d*) was altered less. The subunits ended up looking more similar to each other, with the cavities becoming less prominent due to the fact that they now contained ACh. A superficial explanation of these changes is that the α-subunits are initially distorted unequally by their interactions with neighbouring

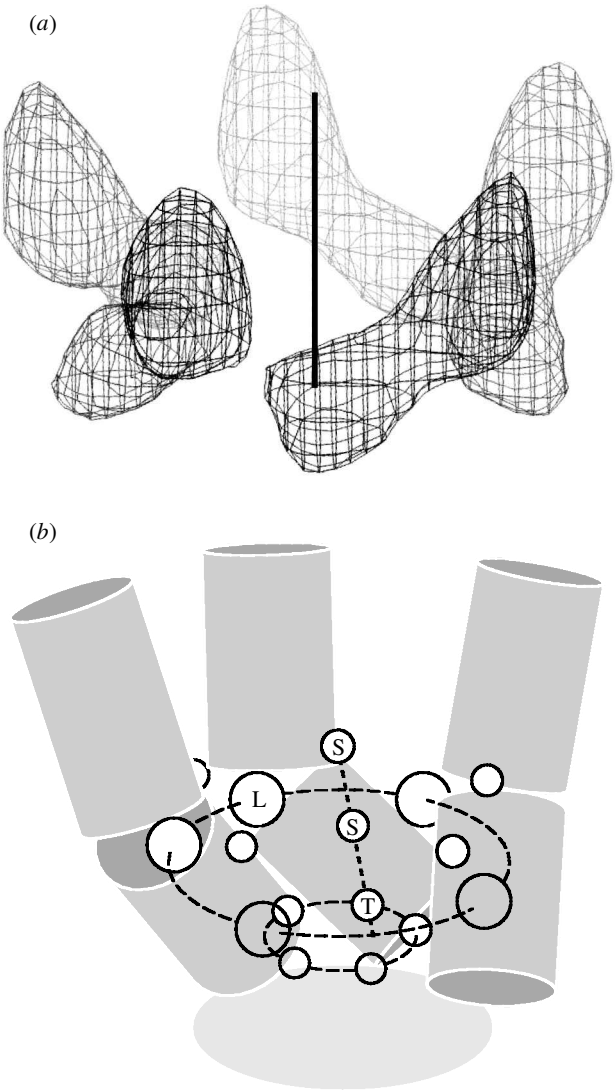

Figure 6. Transient configuration of M2 rods around the open pore, and interpretation at 9 Å. (*a*) A barrel of α-helical segments, having a pronounced twist, forms in the cytoplasmic leaflet of the bilayer, constricting the pore maximally at the cytoplasmic membrane surface. The bend in the rods is at the same level as for the closed pore (see figure 4), but instead of pointing inwards has rotated over to the side. (*b*) Schematic representation of the most distant three rods. A tentative alignment of the amino-acid sequence with the densities suggests that a line of polar residues (serines and threonine; see figure 4*b*) should be facing the open pore. (From Unwin 1995.)

subunits, and that the free energy derived from the binding of two ACh molecules is able to partially overcome these distortions, making the conformations of the subunits more nearly equal.

At the time of this work, in 1995, we could not clearly resolve tunnels that lead into, and out of the cavities, and therefore provide routes by which the ACh can access or leave the binding pockets. These tunnels, and the differences in conformation of the α-subunits around the pockets, are central to our present understanding of how the receptor functions as a gated ion channel, and I will describe them in some detail later.

Comparison of the two maps also suggested that there were small rotations of the subunits (mainly of

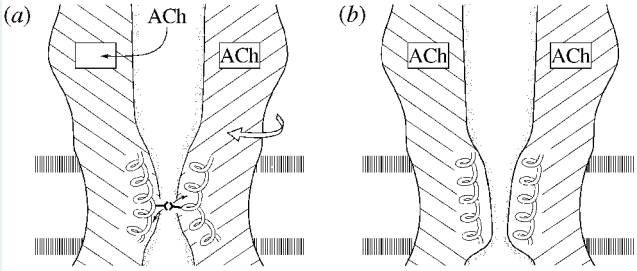

Figure 7. Schematic drawing of the opening mechanism suggested by the freeze-trapping experiments. Binding of ACh to both α-subunits initiates a concerted disturbance at the level of the binding pockets, which leads to small (clockwise) rotations of the α-subunits at the level of the membrane. The rotations destabilize the association of bent α-helices forming the gate, and favour the alternative mode of association (figure 6), in which the pore is wider at the middle of the membrane and most constricted at the cytoplasmic membrane surface. (Adapted from Unwin 1998.)

the α-subunits) linking the disturbances around the binding pockets to the membrane-spanning part of the receptor. In the membrane, the exposure to ACh did not bring about any obvious alteration of the rim of density facing the lipids, whereas the M2 rods switched quite dramatically to a new configuration in which the bends, instead of pointing towards the axis of the pore, had rotated over to the side. As figure 5 shows, the pore was opened up in the middle of the membrane as a result of this action, increasing its diameter there by *ca.* 4 Å.

In the cytoplasmic leaflet, the configuration of M2 rods around the open pore consisted of a 'barrel' of α-helical segments (figure 6*a*), resembling the right-handed twisted barrels of pore-lining α-helices found in the bacterial toxin B-pentamers (Merritt & Hol 1995) and the mechanosensitive channel, MscL (Chang *et al.* 1998). However, in the case of the receptor, the α-helical arrangement gave the pore a strongly tapered shape, making it most constricted at the cytoplasmic membrane surface. Furthermore, only the lower portions of the α-helices came close enough to each other to be stabilized by side-to-side interactions around the ring. This limited association, combined with the rigidity of a barrel, might be important in ensuring both precise permeation and fast gating kinetics.

A tentative alignment of the densities in the cytoplasmic leaflet with the M2 sequence suggested that a line of small polar (serine or threonine) residues would lie almost parallel to the axis of the pore when the channel opens (figure 6*b*), an orientation that should stabilize the passing ions by providing an environment of high polarizability. The threonine residue at the point of maximum constriction (*Torpedo* αThr244), when substituted by other residues of different volume, has a pronounced effect on ion flow, as if it is at the narrowest part of the open pore (Imoto *et al.* 1991; Villarroel *et al.* 1991). Mutagenesis experiments conducted on residues in the loop next to the threonine residue also emphasize the critical nature of this region (Wilson & Karlin 1998; Corringer *et al.* 1999), although the effect of the substitutions and/or insertions

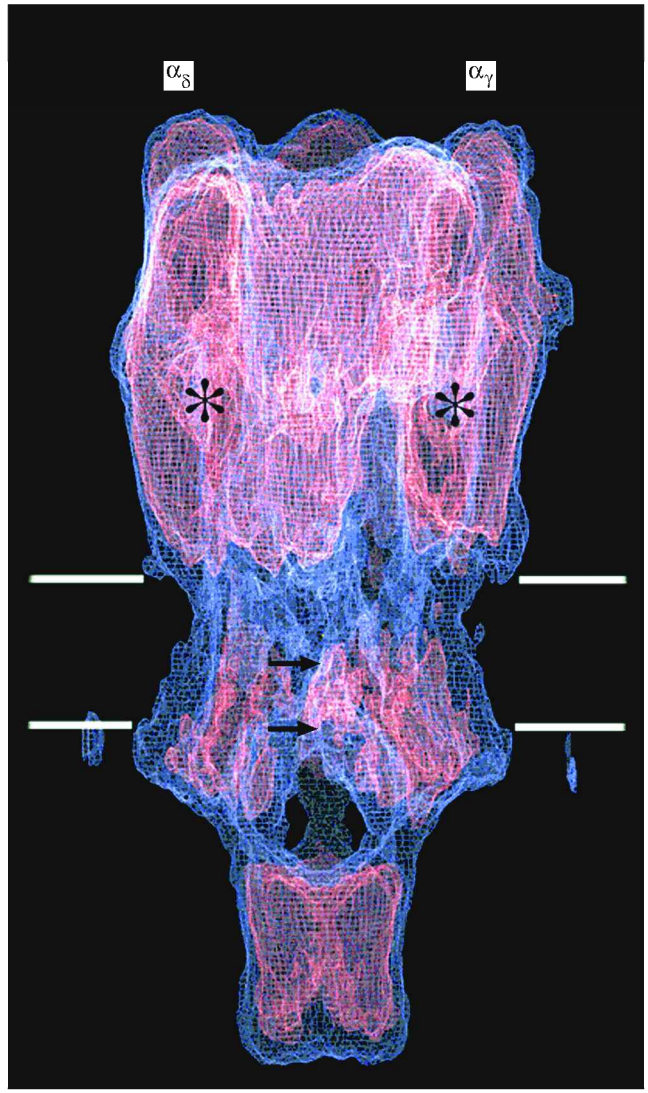

Figure 8. Architecture of whole receptor, emphasizing the external surface and openings to the ion-conducting pathway on the extracellular and cytoplasmic sides of the membrane. The positions of the two α-subunits, the binding pockets (asterisks), gate of the closed channel (upper arrow) and the constricting part of the open channel (lower arrow) are indicated. The subunits are slightly tilted around the axis of the receptor; thus it is the α_δ-subunit that can be seen through the 'window' in the wall of the cytoplasmic vestibule at the back of the receptor.

on the folding of this sensitive part of the protein are unknown.

A simple mechanistic picture of the structural transition, obtained from the study of the activated receptor, was as follows (figure 7). First, ACh triggers distinct, localized disturbances at the binding sites in the two α-subunits. Second, the effects of these of these disturbances are communicated, through small rotations of the α-subunits, to the structure in the membrane. Third, the M2 segments in the membrane transmit the rotations to the gate-forming side-chains, drawing them away from the central axis; the mode of association near the middle of the membrane is thereby disfavoured, and the segments switch to the alternative side-to-side mode of association, creating an open pore.

PHILOSOPHICAL TRANSACTIONS OF THE ROYAL SOCIETY B BIOLOGICAL SCIENCES

PHILOSOPHICAL TRANSACTIONS OF THE ROYAL SOCIETY B BIOLOGICAL SCIENCES

8. ACh RECEPTOR AT HIGHER RESOLUTION

The resolution has been extended recently to about 4 Å, as a result of further averaging (*ca.* 800 000 receptors) and by incorporating the technical improvements I mentioned earlier. This allows a more accurate description of the channel-opening mechanism, and other properties of the receptor, than was possible when the earlier (9 Å) work was published, and brings the analysis close to answering definitively some fundamental questions. For example, how is the cation-selectivity achieved? What is the construction of the gate? How does ACh get into (and out of) the binding pockets? How does the binding of ACh trigger the structural changes that disrupt the gate?

Before going into these questions and describing some of the higher resolution features, first I should summarize the architecture of the receptor (figure 8). The whole complex is *ca.* 160 Å long, and has pseudo-fivefold symmetry over its entire length, except for last *ca.* 20 Å of its cytoplasmic end, which may belong to rapsyn (Miyazawa *et al.* 1999). The extracellular vestibule is a *ca.* 65 Å long, 20 Å wide tube, whereas the cytoplasmic vestibule approximates to a 20 Å diameter sphere (giving rise to a circular outline in the figure). The only aqueous links between the cytoplasmic vestibule and the cell interior are narrow (< 8–9 Å wide) openings in the wall lying directly under the membrane surface. (The cytoplasmic structure of the voltage-gated K^+ channel may have a similar design; Gulbis *et al.* 2000.)

Individual subunits make tight contacts in the upper portion of the extracellular domain and within the membrane, and it will not be possible to determine their exact boundaries in these regions until the polypeptide chains are completely traced. However, the two α-subunits can be identified unambiguously, in other regions, because of their clear structural similarities. Thus it can be shown that the subunits have a small (*ca.* 10°) tilt tangential to the axis of the receptor, giving the whole complex a slightly (right-handed) coiled configuration.

The locations of the two α-subunits, α_δ and α_γ, are indicated in the figure. The δ-subunit lies anticlockwise of α_δ, next to the symmetry axis of the receptor dimer. The single subunit separating the two αs resembles the αs more closely than the others, and so is likely to be β, the subunit having highest sequence homology to α (see also Kubalek *et al.* 1987). However, the interpretation usually given favours γ in this location (Karlin 1993).

The ACh-binding pockets are located about halfway between the extracellular ends of the α-subunits and the membrane (asterisks, figure 8); the gate of the closed pore is near the middle of the membrane (upper arrow, figure 8); and the constricting part of the open pore is at the cytoplasmic membrane surface (lower arrow, figure 8).

9. THE VESTIBULES

Neurotransmitter-gated ion channels have evolved to contain large vestibules, shaped by more than 70% of the total protein mass. Much of this mass extending from the membrane may be involved in shaping the ACh-binding pockets and sites of attachment for regulatory molecules and other proteins (e.g. rapsyn) that are concentrated at the synapse. However, an important physiological function of these vestibules may also be to serve as preselectivity filters, making use of charged groups at their mouths and on their inner walls to electrostatically guide and concentrate the ions they select for while screening out the ions they discriminate against. The ionic environment would consequently be modified close to the narrow membrane-spanning pore, increasing the efficiency of transport of the permeant ions, and enhancing the selectivity arising from their direct interaction with residues and/or backbone groups lining the constriction zone.

Although we will need to see the whole receptor in atomic detail before we know precisely the strategic locations of the charged groups influencing its cation selectivity, some features of the cytoplasmic vestibule already apparent highlight the probable importance of the preselection process. The narrow openings into this vestibule are made between *ca.* 30 Å long α-helices extending down from the base of each subunit and coming together on the central axis of the receptor, forming an inverted pentagonal cone. Clearly these openings would serve as molecular sieves, preventing impermeant cytoplasmic molecules from reaching the vicinity of the pore. However, a stretch of the polypeptide chains between M3 and M4, containing heptad repeats of negatively charged residues, can be identified with the 30 Å long α-helices (Miyazawa *et al.* 1999), and traced tentatively through the 3D densities. The repeating residues are found to line the sides of the openings; moreover, this stretch of amino acids contains additional negatively charged residues which line the vestibule's inner wall. Passing ions must be strongly influenced by these charges, especially at the openings, the widest dimensions of which do not exceed significantly the diameter of an ion including its first hydration shell. On this side of the membrane, therefore, the receptor creates a cation-stabilizing environment, and seems designed largely to exclude anions from the vicinity of the pore.

The extracellular vestibule is architecturally distinct from the cytoplasmic vestibule, yet presumably it participates similarly as a preselectivity filter, since electrophysiological experiments have shown that there is no marked preference for cations to go in one direction across the membrane. It is notable that the cylindrical shape and *ca.* 10 Å radius would provide a route that is narrow enough for the charged groups on the inner wall to influence ions at the centre but not too narrow to restrict their diffusion. The average net negative charge per subunit in the extracellular part of the receptor, estimated from the amino-acid sequences, is −11 e (Unwin 1989). This figure is the same as that for the fast-acting enzyme, acetylcholinesterase from *Torpedo* (Nolte *et al.* 1980; Ripoll *et al.* 1993), where the whole protein surface plays a role in producing an electrostatic field that guides the positively charged ACh substrate to the active site. It is easy to imagine that the receptor uses its predominantly negatively charged surface to guide the ACh molecules and the inorganic cations in a similar fashion (for example, see Adcock *et al.* 1998).

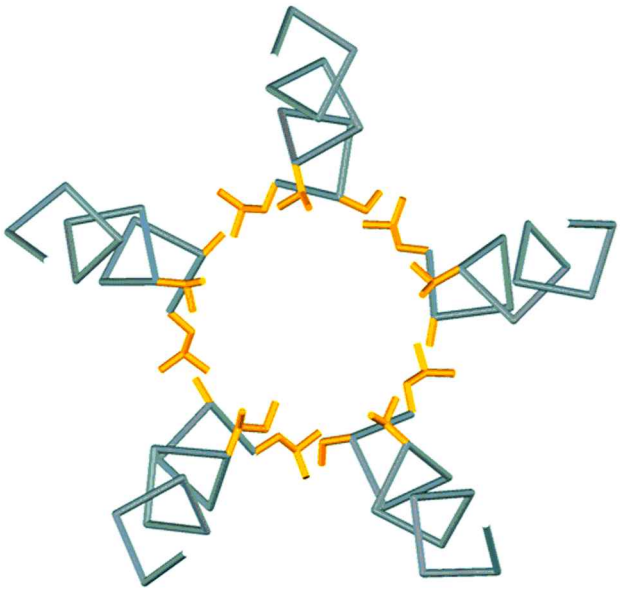

Figure 9. The higher resolution maps suggest that the gate may be made by leucine and valine side-chains creating a hydrophobic girdle around the pore. In the absence of polar groups to provide electrostatic stabilization, the ion would retain its hydration shell and then be too large to pass through the central hole.

10. THE GATE

The gate of the channel lies at the centre of the ring of five bent M2 α-helical segments where they come closest to the axis of the membrane-spanning pore. In the 4.6 Å resolution map of the closed-channel form of the receptor, it is seen as a narrow strip of density—no more than two rings of side-chains thick—bridging the pore (Miyazawa *et al.* 1999). The level of the bridging density is near the middle of the membrane (Unwin 1993), where the dielectric barrier to ion permeation is greatest (Parsegian 1969; Roux & MacKinnon 1999).

The precise nature of the gate—whether it forms a physical occlusion, or is better described as a zone of low polarizability that reinforces the dielectric barrier to ion permeation—has not yet been clarified. Earlier studies (figure 4) had emphasized the likely importance of the ring of conserved leucine residues (αLeu251), and had suggested they might project inwards from the M2 segments, associating side-to-side to form an occluding gate. But the side-chain densities in the higher resolution maps do not come close enough to the pore axis to account for such a simple arrangement.

Apparently there is a hole of *ca.* 3.5 Å radius along the central axis of the pore where the gate is located. This is only slightly smaller than the radius of a Na^+ or K^+ ion having a single hydration shell. Therefore, to be effective in preventing ion permeation, the gate should counter any opportunity for electrostatic stabilization by polar groups that could liberate the ions from their hydration shells. It needs to form a completely hydrophobic girdle around the hole. Two rings of hydrophobic residues could be part of this girdle: one including the conserved leucine and the other including a valine (αVal255; also highly conserved in ACh receptors), one turn of a helix away. Residues in both these rings can be labelled by small uncharged photoactivable compounds when the channel is closed (White & Cohen 1992; Blanton *et al.* 1998).

Figure 9 shows how the leucines may interact side-to-side with alanine and/or serine residues on neighbouring M2 segments, rather than with each other, to form the hydrophobic girdle. Since the M2 segments are not closely packed and draw away from the pore axis and hence from each other on either side of the bend, this may well be the only set of interactions between these segments. The resulting limited stability of the structure would ensure its easy disruption and reassembly by conformational changes initiated at the binding sites.

Other pentameric structures composed of bundles of α-helices, such as phospholamban (Adams *et al.* 1995), the matrix protein COMP (Malashkevich *et al.* 1996) and the mechanosensitive channel (Chang *et al.* 1998), all contain rings of hydrophobic side-chains lying closer to the pore axis than those of the receptor. These side-chains could function as occluding gates. However, the α-helical bundle structures involve more extensive side-to-side interactions, increasing their stability and making them less suited for rapid conversion between two widely distinct and precisely defined states.

The proposed hydrophobic girdle of the ACh receptor contrasts with the central region of the K^+ channel, where there is a large (*ca.* 5 Å radius) water-filled cavity and helix dipoles positioned so as to overcome electrostatic destabilization of the ion (Doyle *et al.* 1998). However, the M2 segments move *ca.* 2 Å away from the pore axis in the middle of the membrane when the channel opens (figure 5). The two central regions would therefore have similar dimensions if the comparison were made with the receptor in the open-channel form.

11. ACh-BINDING POCKETS

The cavities making the ACh-binding pockets lie within the α-subunits about 45 Å away from the gate. At 4.6 Å resolution, narrow tunnels can be seen connecting the cavities to the extracellular vestibule (figure 10; Miyazawa *et al.* 1999). These tunnels, which are 10–15 Å long, are shaped largely by twisted β-sheet strands, and open into the upper (furthest from the membrane) ends of the cavities. The tunnels very likely represent the primary entry routes for ACh into the binding pockets, first because the electrostatic field would favour its movement, along with the inorganic cations, into the vestibule, and second because the tunnel–cavity design parallels the ACh-binding region of acetylcholinesterase, consisting of a narrow 'gorge' about 20 Å long widening out into the active site at its base (Sussman *et al.* 1991). The gorge facilitates the rapid transfer of ACh into the active site, and the tunnels of the receptor would presumably function in an analogous way.

Although the cavities themselves lie entirely within the α-subunits (see below), side-chains from neighbouring δ- and γ-subunits may well make up part of the structure shaping the tunnels and other regions of the vestibule in the vicinity of the cavities. Non α-subunits are indeed likely to participate in the process by which ACh is selectively guided into the binding pocket by contributing charged groups in strategic locations or aromatic side-chains that interact selectively with the quaternary

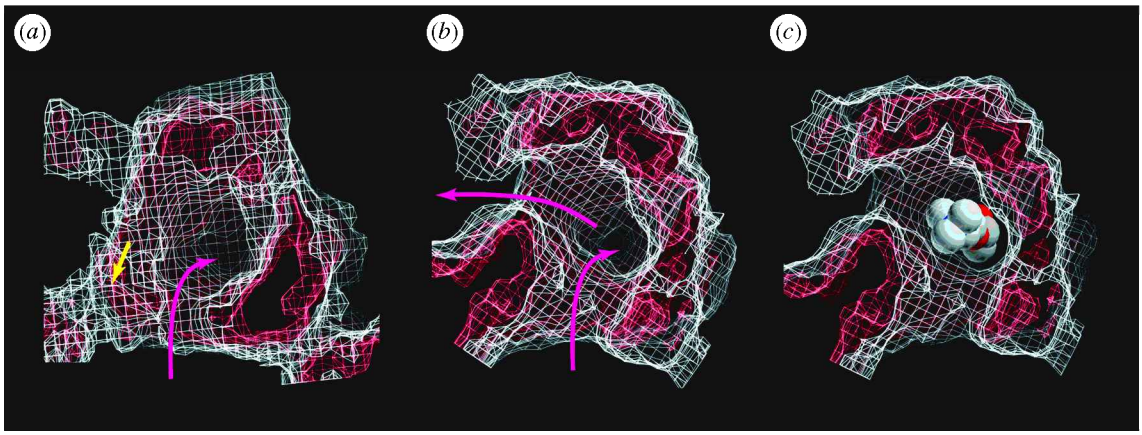

Figure 10. Detail at 4.6 Å resolution showing tunnels at the top of the cavities forming the ACh-binding pockets. (*a*) α_δ contains an 'entry' tunnel (red arrow) connecting to the water-filled vestibule (bottom); (*b*) α_γ contains another tunnel (horizontal red arrow) in addition to the entry tunnel, which may serve as a route for release of ACh into the external surroundings; (*c*) ACh molecule seated in the α_γ-pocket. The α_δ-pocket is more symmetrical and tighter than the α_γ-pocket because of the interaction of α_δ with the neighbouring δ-subunit (indicated by the yellow arrow in (*a*); see § 11).

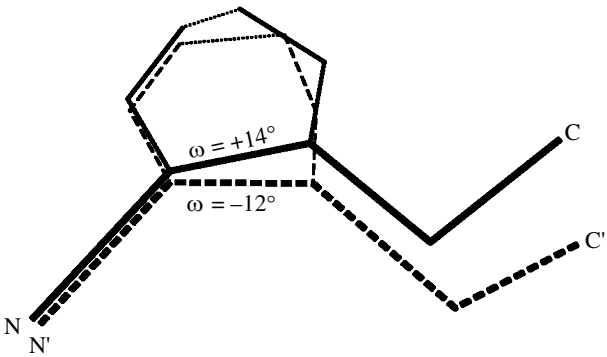

Figure 11. α-carbon tracing of a polypeptide chain containing a pair of adjacent cysteine residues cross-linked to each other in the alternative right-handed (broken line) and left-handed (full line) conformations. The two conformations make different bends in the polypeptide chain. (The torsion angles, ω, of the included *cis* peptide bond are indicated.)

ammonium group (Ripoll *et al.* 1993). These interactions, next to the site where ACh finally resides, may account for some of the chemical labelling and site-directed mutagenesis results interpreted to indicate that the binding sites lie at the α–γ and α–δ interfaces (Czajkowski & Karlin 1995; Sine *et al.* 1995; Chiara & Cohen 1997; Changeux & Edelstein 1998).

In addition to the 'entry' tunnel, α_γ contains another tunnel, at a level slightly closer to the membrane, connecting the binding pocket to the external surroundings (dotted line, figure 3; figure 10*b*). This may serve as an alternative route through which the ACh can be released. Although α_δ does not contain an equivalent tunnel in the absence of ACh (figure 10*a*), both subunits adopt a conformation resembling that of α_γ when ACh is present (+ACh, figure 3). An 'exit' tunnel may therefore appear in α_δ once ACh has bound.

The different conformations of α_δ and α_γ around the cavities, before activation, were apparent from the non-equivalent orientations of the three surrounding rods of density (−ACh, figure 3). At higher resolution, it

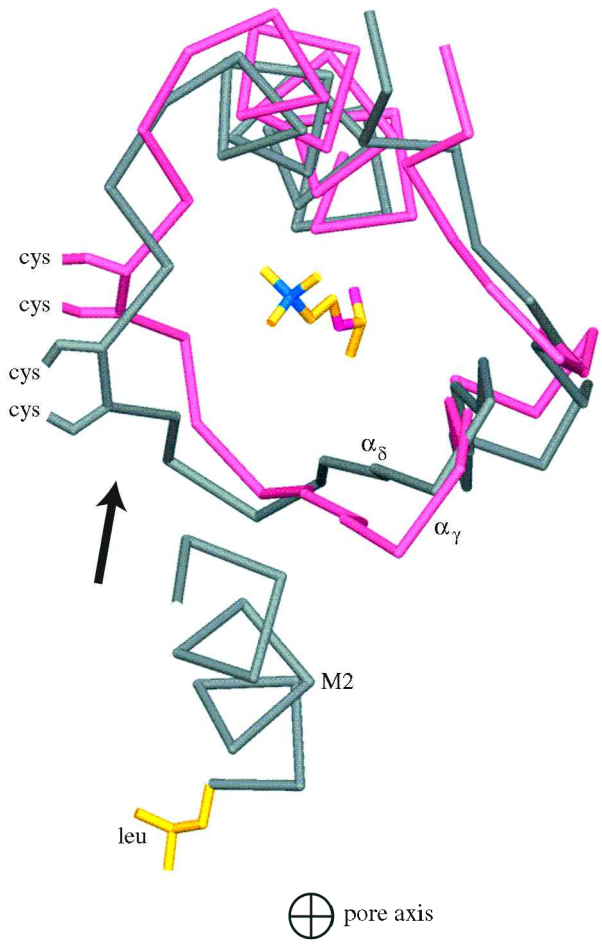

Figure 12. Hypothetical molecular switch controlling activation. Tentative α-carbon tracings are shown of the α_δ- and α_γ-chains (*Torpedo* α166-211) around an ACh molecule in the binding pocket; differences between the two tracings resemble the differences between α_δ before (grey) and after (pink) activation (see figure 3). The comparison suggests that ACh-binding might induce displacements near the pair of cysteine residues (arrow), which in turn might be linked to M2, drawing the gate-forming leucine side-chain away from the axis of the pore. The view is normal to the plane of the membrane.

appears that α_δ creates a more symmetrical and 'tighter' cavity (figure 10*a*) than the one in α_γ (figure 10*b*), because the α_δ-subunit in this region is 'pulled' towards the δ-subunit (yellow arrow, figure 10*a*). The (conical) shapes of the two cavities are quite similar and complement well the Van der Waal's surfaces of the ACh molecule when it is seated slightly tilted with the quaternary ammonium group uppermost (figure 10*c*). In this orientation, the angle formed by the quaternary ammonium group and the membrane normal is about 45°, in agreement with the result obtained by solid-state nuclear magnetic resonance (Williamson *et al*. 2000).

The stretch of polypeptide immediately preceding M1 (*Torpedo* α166–211) can now be traced tentatively though the densities composing the two α-subunits, and shown to be involved in shaping the cavity wall. Thus the cavity-lining rod furthest from the receptor axis (figure 3) is an α-helix that extends down to the membrane surface. Tyr198, which can be photolabelled by the agonist nicotine (Middleton & Cohen 1991), is at the upper end of the helix and faces the cavity. This whole stretch of polypeptide chain encircles the cavity, and contains a β-sheet hairpin opposite the α-helix, which draws away from the helix in the upper portion, defining the cavity space.

12. A HYPOTHETICAL SWITCH CONTROLLING ACTIVATION

Biophysical evidence has shown that ACh receptor behaves as an allosteric protein, undergoing concerted 'all or none' transitions consistent with the Monod–Wyman–Changeux model (Monod *et al*. 1965). For example, the channels occasionally open spontaneously, and do so with the same conductance properties as the ACh-activated channels (Jackson 1994). It appears that the protein interconverts between two discrete 'pre-existing' closed- and open-channel forms, and that ACh binding simply alters the equilibrium in favour of the open-channel form. The alternative forms of an allosteric protein are often described in terms of a tense, or T state, where a subunit is constrained to resist the change needed for ligand binding, and a relaxed, or R state, where these constraints are relieved. This description also readily applies to the receptor. The structures shaping the two binding pockets in the α-subunits are not equivalent initially (despite their compositions being the same) because of the unequal constraints imposed by interactions with different neighbouring subunits. So the receptor is initially in the T state. However, the two structures become more similar upon activation, indicating that the binding of ACh (partially) overcomes these constraints. The receptor therefore changes into a less distorted conformation, which is closer to the R state.

The α_δ-binding region is the one changed most by the allosteric transition, and ends up resembling the binding region of α_γ in the initial state (see figure 3). How does ACh convert α_δ into the activated conformation resembling α_γ? The structural results point to a critical role played by the adjacent cysteines, αCys192 and αCys193, which are at the periphery of the binding site close to the δ–α-subunit interface (Kao *et al*. 1984; Czajkowski & Karlin 1995). Arthur Karlin and his colleagues showed that these cysteines are cross-linked to each other, forcing a non-planar *cis*, rather than the normal *trans* peptide bond. They suggested that the binding of ACh may initiate a conversion between two stable conformations of the disulphide and peptide bonds (Chandrasekaran & Balasubramanian 1969), so that Cys192–193 acts as a molecular switch controlling receptor activation (Kao & Karlin 1986). How might this switch trigger the observed structural change? As figure 11 shows, the alternative *cis* conformations make different bends in the polypeptide chain. Entry of an ACh molecule into the tighter α_δ-pocket (figure 10*a*) might therefore trigger the change by stabilizing the less bent *cis* conformation which, in turn, would resist the constraint imposed by the δ-subunit to produce a more extended configuration of the polypeptide chain.

A comparison of the α_δ and α_γ polypeptide configurations in the ACh-binding region, before activation, gives some insight into the possible physical nature of this switch. Figure 12 shows the two chains superimposed (after rotating one subunit by 144° relative to the other). Assuming now that the α_γ configuration is a good approximation to activated α_δ, the structural change would entail some reorientation of the α-helix and some displacement of the β-hairpin and the rest of the chain. In fact, a small overall (clockwise) twist is produced, which might be the origin of the subunit rotation detected earlier (figure 7). Most significant is the *ca*. 3 Å displacement near the pair of cysteine residues, which is approximately in the direction (arrow) that would counter the distortion imposed by the δ-subunit.

The extracellular (C-terminal) end of the M2 segment lies close in projection to the pair of cysteines (figure 12) and, therefore, so does the loop, M2–M3, implicated in the control of gating (Grosman *et al*. 2000). It is plausible then that this displacement initiated near the pair of cysteines would be transmitted to the M2 segment and move it away from the axis of the pore. Although the concerted transition to open the channel involves structural changes in all five subunits (Unwin 1995), not all M2 segments need directed motion to destabilize the gate and favour the open configuration around the pore. A structural link between the binding site and gate, like that depicted in figure 12, might therefore function as a 'communicating arm', exerting physiological control by modulating the relative stabilities of the closed and open configurations in the membrane.

13. PORE-OPENING MECHANISM

The earlier electron microscopical experiments highlighted the role of the M2 segments, not only as the main structural elements lining the pore, but also as dynamic elements effecting its opening or closure. Apparently, these segments move largely independently of the outer lipid-facing rim of protein (figure 5) and switch from one mode of side-to-side association to the other, controlled by the binding of ACh. In the closed-channel form of the receptor, the segments come together near the middle of the membrane to make the gate of the channel and prevent ion permeation. In the open-channel form they come together near the cytoplasmic membrane surface to make the constriction zone, where direct interaction between the hydrated ions and encircling protein

determines most critically whether or not the ions can go through. While we do not understand yet the structural switch controlling the relative stabilities of these two configurations, the higher resolution details point to the importance of the constraints around the ACh-binding pockets, which are relaxed in the open-channel form, and the possibility of a direct link between the binding pocket and M2.

The bend, or kink, near the middle of the M2 segment, seems to play a crucial role in facilitating the rapid switch between the closed and open pore. In acting as a point of flexure, it allows this critical part of the receptor to move economically within the rest of the membrane-spanning structure, so that there is no direct influence on the motion by the surrounding lipids. The bend also gives the segment freedom to move towards or away from the central axis, and so modifies instantly the shape, size and chemical surroundings of the pore. Interestingly, molecular dynamics simulations of isolated α-helices in water show that those composed of the M2 stretch of amino acids have a propensity for localized flexure in their middle portion. The M2 helix unfolds in this region, in the simulations, allowing the bend to act as a molecular swivel, or hinge (Law *et al.* 2000).

This kind of localized movement within the membrane-spanning part of a structure is presumably used also by other neurotransmitter-gated ion channels of the ACh receptor family to alter the dimensions of their pores, and may indeed be a central feature of the activation mechanisms of many proteins involved in transporting ions across the lipid bilayer. Bacteriorhodopsin, a light-driven proton pump, is an example of a well-studied membrane protein where flexure of α-helices about a point near the middle of the membrane has been shown to play an important functional role (Subramaniam & Henderson 2000).

14. RELATED EVENTS AT THE ELECTRICAL SYNAPSE

The electrical synapse is a region of contact between a pair of nerve cells that mediates fast electrical transmission by providing pathways for ion diffusion through connecting gap junction channels. Although less common in the nervous system than the chemical synapse, it is being found in many different parts with increasing frequency (Bennett 2000).

The gap junction channel is built from a ring of six similar, or identical protein subunits, called connexins. The connexins constitute a family of homologous polypeptides that fold to form four-α-helical bundle structures within the lipid bilayer (Unger *et al.* 1999). They are unusual because of their dual role: not only do they associate within the plasma membrane of one cell to make a channel, but they also join to connexins in the plasma membrane of another cell to make a continuous conducting pathway between the two interiors. A widely expressed, 36 kDa neuron-specific connexin has recently been cloned (Condorelli *et al.* 1998; Söhl *et al.* 1998).

Gap junction channels have not been explored in the same detail as the ACh receptor; however, the studies so far carried out suggest that the two channels may have structural parallels and work by similar physical

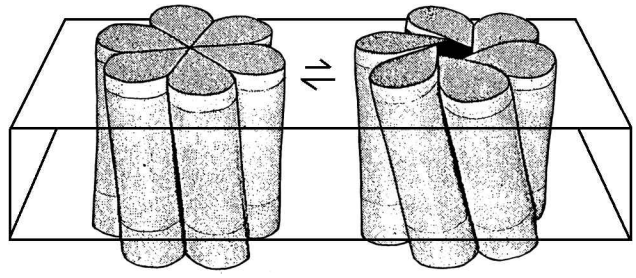

Figure 13. Model for the concerted transition between closed and open forms of the gap junction channel, based on low resolution electron crystallographic studies. Tilting of the protein subunits around the axis of the channel gives rise to small tangential displacements in the plane of the membrane, which combine to make large changes in pore dimensions at the cytoplasmic membrane surface (adapted from Unwin & Zampighi 1980).

principles. The putative pore-lining segment, M3, has a similar pattern of bulky hydrophobic and small polar residues as M2 of the ACh receptor, and there is a conserved phenylalanine in place of αLeu251 (Unwin 1989). But the gap junction pore is wider and less selective, allowing the passage of small molecules (<1–2 kDa), as well as ions, between connected cells. Also gap junction channels do not desensitize, making it possible to stabilize either the closed- or open-channel form simply by using different concentrations of ligand. High concentrations of Ca^{2+} and H^+ ions lead to rapid closure (Rose & Loewenstein 1977; Spray *et al.* 1981).

Since the gating mechanism of the gap junction channel involves large changes in pore dimensions, the accompanying conformational change should be detectable even at low resolution. Electron crystallographic studies (Unwin & Zampighi 1980) and low-angle X-ray diffraction experiments (Unwin & Ennis 1983), conducted on isolated gap junctions, have shown that there are indeed two alternative arrangements of the protein subunits around the pore (figure 13). At high [Ca^{2+}], where the channel should be closed, the subunits are orientated approximately parallel to the pore axis; while at low [Ca^{2+}], where the channel should be open, they are inclined tangentially to this axis. The lowered [Ca^{2+}] widens the pore at the cytoplasmic membrane surface in proportion to this change in tilt (Unwin & Ennis 1984).

The gap junction and the ACh receptor channels therefore both use coordinated tilting of α-helical segments around the pore to bring about changes in its properties. In both cases the tilt axes lie approximately parallel to the membrane plane, creating displacements predominantly within the plane that keep the same polar and hydrophobic surfaces exposed to water, protein and lipid. This kind of rearrangement, common to both channels, is energetically favourable and efficient in terms of minimizing perturbation of the structure to achieve maximum effect. Small in-plane displacements of individual α-helices or subunits around a pore combine to alter significantly its size and ability to stabilize the ions, because they expose different sets of amino-acid side-chains and/or backbone groups to the lumen and introduce new physically and chemically distinct surfaces.

A recent analysis by electron paramagnetic resonance spectroscopy of the KscA channel (Perozo *et al.* 1999), suggested that the membrane-spanning α-helices of K^+ channels may move according to these principles, upon activation, to change the properties of the pore. The same might therefore be said about the synaptic channels gated by glutamate, which are related in sequence to K^+ channels (Chen *et al.* 1999).

15. CONCLUSIONS

Release of chemical transmitter at the nerve terminal leads to a fast, predictable electrical response at the postsynaptic membrane of the target cell, which is mediated by the rapid and robust action of ion-selective neurotransmitter-gated channels. Many of the principles underlying the behaviour of these channels are probably quite general and shared with the ACh receptor, the only neurotransmitter-gated channel for which a 3D structure is available. The structures I have described of this protein suggest that interaction of neurotransmitter with its receptor sets in train a number of events, involving all subunits, which are distributed over the length of the channel.

The ACh receptor-mediated events might be summarized as follows. ACh molecules are drawn electrostatically into the mouth of the extracellular vestibule and selectively guided through tunnels in the wall to pockets located within both α-subunits. The free energy of binding then triggers a concerted allosteric transition by a mechanism in which the two adjacent α-subunit cysteines may play a key role. All subunits are affected, enabling the α-subunits to overcome the constraints imposed on them by neighbouring subunits and become more nearly equivalent. The conformational change produces a twisting of the α-subunit between the binding pocket and the membrane, which is communicated to the membrane-spanning segment, M2, drawing it away from the lumen of the pore. This weakens the stability of the hydrophobic girdle, forming the gate near the middle of the membrane, in favour of the alternative 'open' configuration of M2 segments where the pore is wider near the middle of the membrane and most constricted at the cytoplasmic membrane surface. The selected ions now pass readily across the membrane because the pore has a short constriction lined by polar residues, instead of the hydrophobic barrier, and because ions of the right charge have been concentrated relative to those of the wrong charge by preselection through the vestibules. Initially, the driving force is mainly for Na^+ ions from the outside to flow into the cell but, as the membrane depolarizes, an increasing proportion of K^+ ions flow in the opposite direction. Soon, after a millisecond or so, the weakly bound ACh molecules are released from their binding pockets into the now ACh-depleted surroundings, the transient open-channel structure is no longer favoured and the receptor returns to its original non-conducting state.

I have also described briefly some properties of the gap junction channel, the relatively non-selective channel mediating fast electrical synaptic transmission. The structural rearrangements around the pore of this protein were seen to be analogous to those of the receptor, entailing changes that can readily be accommodated in the two phase water–lipid environment. Both channels use co-ordinated lateral motions in the membrane, developed by tilting of α-helical segments, to effect opening and closure of the pore. It would not be surprising if all fast synaptic transmission is mediated by this same general mechanism.

Despite the progress made over the past 40 years in visualizing events and in determining the molecular properties underlying the fast postsynaptic response, we still only have a fairly elementary picture through the example of the ACh receptor. It would be valuable to know the precise organization of amino-acid side-chains in the vicinity of the ACh-binding pockets, so that the binding reaction could be better understood. Knowledge of the folding of the polypeptide chains extending from the binding region to the membrane would allow a more complete account of the coordinated ligand–receptor action controlling the stability of the gate. Insight with wide implications would be obtained by defining the protein scaffold that partitions the moving pore-lining helices away from the lipids; does this membrane-spanning motif entail subunit–subunit interactions through the polypeptide backbone groups, which would maintain a constant 3D framework so that alternative subunits can be precisely 'slotted in'? An exact localization of charged, polar and hydrophobic groups would enable a quantitative description of the electrostatic influences on ion-selectivity and the rate of transport through the pore. Fortunately an atomic model of the ACh receptor seems not too far away. It should help in extending significantly our understanding not only of this ion channel, but also of others at the synapse, and elsewhere.

All the more recent work has been conducted in collaboration with Professor Yoshi Fujiyoshi, making use of his highly stable, liquid helium-cooled microscope stage. To him I owe special thanks. I am also fortunate to have worked closely with many other outstanding colleagues at the MRC Laboratory of Molecular Biology, Cambridge, UK, the Scripps Research Institute, La Jolla, CA, USA and Kyoto University, Japan whose advice, collaboration and support have strongly influenced the course of this work. The staff of the Marine Station at Roscoff, France are warmly thanked for their continued interest and for the frequent supply of *Torpedo marmorata* electric rays. The research has been supported in part by grants from the US National Institutes of Health and the European Commission, and by funds from the Louis Jeantet Foundation, Geneva, Switzerland.

REFERENCES

Adams, P. D., Arkin, I. T., Engelman, D. M. & Brunger, A. T. 1995 Computational searching and mutagenesis suggest a structure for the pentameric transmembrane domain of phospholamban. *Nature Struct. Biol.* **2**, 154–162.

Adcock, C., Smith, G. R. & Sansom, M. S. P. 1998 Electrostatics and ion selectivity of ligand-gated channels. *Biophys. J.* **75**, 1211–1222.

Bennett, M. V. L. 2000 Seeing is relieving: electrical synapses between visualized neurons. *Nature Neurosci.* **3**, 7–9.

Beroukhim, R. & Unwin, N. 1997 Distortion correction of tubular crystals: improvements in the acetylcholine receptor structure. *Ultramicroscopy* **70**, 57–81.

Berriman, J. & Unwin, N. 1994 Analysis of transient structures by cryo-microscopy combined with rapid mixing of spray droplets. *Ultramicroscopy* **56**, 241–252.

Blanton, M. P., Dangott, L. J., Raja, S. K., Lala, A. K. & Cohen, J. B. 1998 Probing the structure of the nicotinic acetylcholine receptor ion channel with the uncharged photoactivable compound [3H]diazofluorene. *J. Biol. Chem.* **273**, 8659–8668.

Brisson, A. & Unwin, P. N. T. 1984 Tubular crystals of acetylcholine receptor. *J. Cell Biol.* **99**, 1202–1211.

Brisson, A. & Unwin, P. N. T. 1985 Quaternary structure of the acetylcholine receptor. *Nature* **315**, 474–477.

Chandrasekaran, R. & Balasubramanian, R. 1969 Stereochemical studies of cyclic peptides. VI. Energy calculations of the cyclic disulphide cysteinyl-cysteine. *Biochim. Biophys. Acta* **188**, 1–9.

Chang, H. W. & Bock, E. 1977 Molecular forms of acetylcholine receptor. Effects of calcium ions and a sulfhydryl reagent on the occurrence of oligomers. *Biochemistry* **16**, 4513–4520.

Chang, G., Spencer, R. H., Lee, A. T., Barclay, M. T. & Rees, D. C. 1998 Structure of the MsL homolog from *Mycobacterium tuberculosis*: a gated mechanosensitive ion channel. *Science* **282**, 2220–2226.

Changeux, J.-P. & Edelstein, S. J. 1998 Allosteric receptors after 30 years. *Neuron* **21**, 959–980.

Charnet, P., Labarca, C., Leonard, R. J., Vogelaar, N. J., Czyzyk, L., Gowin, A., Davidson, N. & Lester, H. A. 1990 An open-channel blocker interacts with adjacent turns of α-helices in the nicotinic acetylcholine receptor. *Neuron* **4**, 87–95.

Chen, G.-Q., Cui, C., Mayer, M. L. & Gouaux, E. 1999 Functional characterization of a potassium-selective prokaryotic glutamate receptor. *Nature* **402**, 817–821.

Chiara, D. C. & Cohen, J. B. 1997 Identification of amino acids contributing to high and low affinity *d*-tubocurarine sites in the *Torpedo* nicotinic acetylcholine receptor. *J. Biol. Chem.* **272**, 32 940–32 950.

Colquhoun, D. & Sakmann, B. 1985 Fast events in single-channel currents activated by acetylcholine and its analogues at the frog muscle end-plate. *J. Physiol. (Lond.)* **369**, 501–557.

Condorelli, D. F., Parenti, R., Spinella, F., Trovato Salinaro, A., Belluardo, N., Cardile, V. & Cicirata, F. 1998 Cloning of a new gap junction gene (Cx36) highly expressed in mammalian brain neurons. *Eur. J. Neurosci.* **10**, 1202–1208.

Corringer, P.-J., Bertrand, S., Galzi, J.-L., Devillers-Thiery, A., Changeux, J.-P. & Bertrand, D. 1999 Mutational analysis of the charge selectivity filter of the α7 nicotinic acetylcholine receptor. *Neuron* **22**, 831–843.

Craik, C. S., Largman, C., Fletcher, T., Roczniak, S., Barr, P. J., Fletterick, R. & Rutter, W. J. 1985 Redesigning trypsin: alteration of substrate specificity. *Science* **228**, 291–297.

Czajkowski, C. & Karlin, A. 1995 Structure of the nicotinic receptor acetylcholine-binding site. Identification of acidic residues in the δ-subunit within 0.9 nm of the α-subunit binding disulfide. *J. Biol. Chem.* **270**, 3160–3164.

DeRosier, D. J. & Klug, A. 1968 Reconstruction of three-dimensional structures from electron micrographs. *Nature* **217**, 130–134.

DeRosier, D. J. & Moore, P. B. 1970 Reconstruction of three-dimensional images from electron micrographs of structures with helical symmetry. *J. Mol. Biol.* **52**, 355–369.

Doyle, D. A., Cabral, J. M., Pfuetzner, R. A., Kuo, A., Gulbis, J. M., Cohen, S. L., Chait, B. T. & MacKinnon, R. 1998 The structure of the potassium channel: molecular basis of K^+ conduction and selectivity. *Science* **280**, 69–77.

Dubochet, J., Adrian, M., Chang, J.-J., Homo, J.-C., Lepault, J., McDowall, A. W. & Schultz, P. 1988 Cryo-electron microscopy of vitrified specimens. *Q. Rev. Biophys.* **21**, 129–228.

Fernandez-Chacon, R. & Sudhof, T. C. 1999 Genetics of synaptic vesicle function: toward the complete functional anatomy of an organelle. *A. Rev. Physiol.* **61**, 753–776.

Filatov, G. N. & White, M. M. 1995 The role of conserved leucines in the M2 domain of the acetylcholine receptor in channel gating. *Mol. Pharmacol.* **48**, 379–384.

Fujiyoshi, Y. 1998 The structural study of membrane proteins by electron crystallography. *Adv. Biophys.* **35**, 27–74.

Fujiyoshi, Y., Mizuasaki, T., Morikawa, K., Yamagishi, H., Aoki, Y., Kihara, H. & Harada, Y. 1991 Development of a superfluid helium stage for high resolution electron microscopy. *Ultramicroscopy* **38**, 241–251.

Giraudat, J., Dennis, M., Heidmann, T., Chang, J.-Y. & Changeux, J.-P. 1986 Structure of the high affinity site for non-competitive blockers of the acetylcholine receptor: serine-262 of the δ-subunit is labelled by [3H]chlorpromazine. *Proc. Natl Acad. Sci. USA* **83**, 2719–2723.

Grosman, C., Salamone, F. N., Sine, S. M. & Auerbach, A. 2000 The extracellular linker of muscle acetylcholine receptor channels is a gating control element. *J. Gen. Physiol.* **116**, 327–339.

Gulbis, J. M., Zhou, M., Mann, S. & MacKinnon, R. 2000 Structure of the cytoplasmic β-subunit-T1 assembly of voltage-dependent K^+ channels. *Science* **289**, 123–127.

Henderson, R. & Unwin, P. N. T. 1975 Three-dimensional model of purple membrane obtained by electron microscopy. *Nature* **257**, 28–32.

Heuser, J. E. & Salpeter, S. R. 1979 Organization of acetylcholine receptors in quick-frozen, deep-etched, and rotary-replicated *Torpedo* postsynaptic membrane. *J. Cell Biol.* **82**, 150–173.

Heuser, J. E., Reese, T. S., Dennis, M. J., Jan, L., Jan, Y. & Evans, L. 1979 Synaptic vesicle exocytosis captured by quick freezing and correlation with quantal transmitter release. *J. Cell Biol.* **81**, 275–300.

Hille, B. 1992 *Ionic channels of excitable membranes.* Sunderland, MA: Sinauer Associates.

Hucho, F., Oberthur, W. & Lottspeich, F. 1986 The ion channel of the nicotinic acetylcholine receptor is formed by the homologous helices MII of the receptor subunits. *FEBS Lett.* **205**, 137–142.

Imoto, K., Busch, C., Sakmann, B., Mishina, M., Konno, T., Nakai, J., Bujo, H., Mori, Y., Fukuda, K. & Numa, S. 1988 Rings of negatively charged amino acids determine the acetylcholine receptor channel conductance. *Nature* **355**, 645–648.

Imoto, K., Konno, T., Nakai, J., Wang, F., Mishina, M. & Numa, S. 1991 A ring of uncharged polar amino acids as a component of channel constriction in the nicotinic acetylcholine receptor. *FEBS Lett.* **289**, 193–200.

Jackson, M. B. 1994 Single channel currents in the nicotinic acetylcholine receptor: a direct demonstration of allosteric transitions. *Trends Biochem. Sci.* **19**, 396–399.

Kao, P. N. & Karlin, A. 1986 Acetylcholine receptor binding site contains a disulfide cross-link between adjacent half-cystinyl residues. *J. Biol. Chem.* **261**, 8085–8088.

Kao, P. N., Dwork, A. J., Kaldany, R. J., Silver, M. L., Widemann, J., Stein, S. & Karlin, A. 1984 Identification of the α subunit half-cystine specifically labeled by an affinity reagent for the acetylcholine receptor binding site. *J. Biol. Chem.* **259**, 11 662–11 665.

Karlin, A. 1993 Structure of nicotinic acetylcholine receptors. *Curr. Opin. Neurobiol.* **3**, 299–309.

Katz, B. 1962 The transmission of impulses from nerve to muscle, and the subcellular unit of synaptic action. *Proc. R. Soc. Lond.* B **155**, 455–477.

Kistler, J. & Stroud, R. M. 1981 Crystalline arrays of membrane-bound acetylcholine receptor. *Proc. Natl Acad. Sci. USA* **78**, 3678–3682.

Klug, A., Crick, F. H. C. & Wykoff, H. W. 1958 Diffraction by helical structures. *Acta Crystallogr.* **11**, 199–213.

Kubalek, E., Ralston, S., Lindstrom, J. & Unwin, N. 1987 Location of subunits within the acetylcholine receptor by electron image analysis of tubular crystals from *Torpedo marmorata*. *J. Cell Biol.* **105**, 9–18.

Kubo, T. (and 11 others) 1985 Primary structure of α-subunit precursor of calf muscle acetylcholine receptor deduced from cDNA sequence. *Eur. J. Biochem.* **149**, 5–13.

Labarca, C., Nowak, M. W., Zhang, H., Tang, L., Deshpande, P. & Lester, H. A. 1995 Channel gating governed symmetrically by conserved leucine residues in the M2 domain of nicotinic receptors. *Nature* **376**, 514–516.

Law, R. J., Forrest, L. R., Ranatunga, K. M., La Rocca, P., Tieleman, P. & Sansom, S. P. 2000 Structure and dynamics of the pore-lining helix of the nicotinic receptor: MD simulations in water, lipid bilayers and transbilayer bundles. *Proteins* **39**, 47–55.

Leonard, R. J., Labarca, C. G., Charnet, P., Davidson, N. & Lester, H. A. 1988 Evidence that the M2 membrane-spanning region lines the ion channel pore of the nicotinic receptor. *Science* **242**, 1578–1581.

Lepault, J., Booy, F. P. & Dubochet, J. 1983 Electron microscopy of frozen biological suspensions. *J. Microscopy* **129**, 89–102.

McCrea, P. D., Popot, J.-L. & Engelman, D. M. 1987 Transmembrane topography of the nicotinic acetylcholine receptor δ-subunit. *EMBO J.* **6**, 3619–3626.

McLachlan, D. 1958 Crystal structure and information theory. *Proc. Natl Acad. Sci. USA* **44**, 948–956.

Malashkevich, V. N., Kammerer, R. A., Efimov, V. P., Schulthess, T. & Engel, J. 1996 The crystal structure of a five-stranded coiled coil in COMP: a prototype ion channel? *Science* **274**, 761–765.

Marsh, M. & McMahon, H. T. 1999 The structural era of endocytosis. *Science* **285**, 215–220.

Matsubara, N., Billington, A. P. & Hess, G. P. 1992 How fast does an acetylcholine receptor channel open? Laser-pulse photolysis of an inactive precursor of carbamoylcholine in the microsecond time region with BC3H1 cells. *Biochemistry* **31**, 5507–5514.

Merritt, E. A. & Hol, W. G. J. 1995 AB5 toxins. *Curr. Opin. Struct. Biol.* **5**, 165–171.

Middleton, R. E. & Cohen, J. B. 1991 Mapping of the acetylcholine binding site of the nicotinic acetylcholine receptor: [3H]nicotine as an agonist photoaffinity label. *Biochemistry* **30**, 6987–6997.

Mitra, A. K., McCarthy, M. P. & Stroud, R. M. 1989 Three-dimensional structure of the nicotinic acetylcholine receptor and location of the major associated 43 kDa cytoskeletal protein, determined at 22 Å by low dose electron microscopy and X-ray diffraction to 12.5 Å. *J. Cell Biol.* **109**, 755–774.

Miyazawa, A., Fujiyoshi, Y., Stowell, M. & Unwin, N. 1999 Nicotinic acetylcholine receptor at 4.6 Å resolution: transverse tunnels in the channel wall. *J. Mol. Biol.* **288**, 765–786.

Monod, J., Wyman, J. & Changeux, J.-P. 1965 On the nature of allosteric transitions: a plausible model. *J. Mol. Biol.* **12**, 88–118.

Moody, M. F. 1990 Image analysis of electron micrographs. In *Biophysical electron microscopy. Basic concepts and modern techniques* (ed. P. W. Hawkes & U. Valdre), pp. 145–287. London: Academic Press.

Neubig, R. R., Krodel, E. K., Boyd, N. D. & Cohen, J. B. 1979 Acetylcholine and local anaesthetic binding to *Torpedo* nicotinic post-synaptic membranes after removal of non-receptor peptides. *Proc. Natl Acad. Sci. USA* **76**, 690–694.

Nolte, H.-J., Rosenberry, T. L. & Neumann, E. 1980 Effective charge on acetylcholinesterase active sites determined from the ionic strength dependence of association rate constants with cationic ligands. *Biochemistry* **19**, 3705–3711.

Parsegian, A. 1969 Energy of an ion crossing a low dielectric membrane: solutions to four relevant electrostatic problems. *Nature* **221**, 844–846.

Perozo, E., Cortes, D. M. & Cuello, L. G. 1999 Structural rearrangements underlying K^+-channel activation gating. *Science* **285**, 73–78.

Popot, J.-L. & Changeux, J.-P. 1984 Nicotinic receptor of acetylcholine: structure of an oligomeric membrane protein. *Physiol. Rev.* **64**, 1162–1239.

Ripoll, D. R., Faerman, C. H., Axelsen, P. H., Silman, I. & Sussman, J. L. 1993 An electrostatic mechanism for substrate guidance down the aromatic gorge of acetylcholinesterase. *Proc. Natl Acad. Sci. USA* **90**, 5128–5132.

Rose, B. & Loewenstein, W. R. 1977 Permeability of cell junction depends on local cytoplasmic calcium activity. *Nature* **254**, 250–252.

Roux, B. & MacKinnon, R. 1999 The cavity and the pore helices in the KcsA K^+ channel: electrostatic stabilization of monovalent cations. *Science* **285**, 100–102.

Sealock, R., Wray, B. E. & Froehner, S. C. 1984 Ultrastructural localization of the Mr 43 000 protein and the acetylcholine receptor in *Torpedo* postsynaptic membranes using monoclonal antibodies. *J. Cell Biol.* **98**, 2239–2244.

Sine, S. M., Kreienkamp, H.-J., Bren, N., Maeda, R. & Taylor, P. 1995 Molecular dissection of subunit interfaces in the acetylcholine receptor: identification of determinants of α-conotoxin M1 selectivity. *Neuron* **15**, 205–211.

Söhl, G., Degen, J., Teubner, B. & Willecke, K. 1998 The murine gap junction gene connexin36 is highly expressed in mouse retina and regulated during brain development. *FEBS Lett.* **428**, 27–31.

Spray, D. C., Harris, A. L. & Bennett, M. V. L. 1981 Gap junctional conductance is a simple and sensitive function of intracellular pH. *Science* **211**, 712–715.

Subramaniam, S. & Henderson, R. 2000 Molecular mechanism of vectorial translocation by bacteriorhodopsin. *Nature* **406**, 653–657.

Sussman, J. L., Harel, M., Frolow, F., Oefner, C., Goldman, A., Toker, L. & Silman, I. 1991 Atomic structure of acetylcholinesterase from *Torpedo californica:* a prototypic acetylcholine-binding protein. *Science* **253**, 872–878.

Taylor, K. A. & Glaeser, R. M. 1976 Electron microscopy of frozen hydrated biological specimens. *J. Ultrastruct. Res.* **55**, 448–456.

Tierney, L., Birnir, B., Pillai, N. P., Clements, J. D., Howitt, S. M., Cox, G. B. & Gage, P. W. 1996 Effects of mutating leucine to threonine in the M2 segment of the α_1 and β_1 subunits of GABAA $\alpha_1\beta_1$ receptors. *J. Membr. Biol.* **154**, 11–21.

Toyoshima, C. & Unwin, N. 1988 Ion channel of acetylcholine receptor reconstructed from images of postsynaptic membranes. *Nature* **336**, 247–250.

Toyoshima, C. & Unwin, N. 1990 Three-dimensional structure of the acetylcholine receptor by cryoelectron microscopy and helical image reconstruction. *J. Cell Biol.* **111**, 2623–2635.

Unger, V. M., Kumar, N. M., Gilula, N. B. & Yeager, M. 1999 Three-dimensional structure of a recombinant gap junction membrane channel. *Science* **283**, 1176–1180.

Unwin, N. 1989 The structure of ion channels in membranes of excitable cells. *Neuron* **3**, 665–676.

Unwin, N. 1993 Nicotinic acetylcholine receptor at 9 Å resolution. *J. Mol. Biol.* **229**, 1101–1124.

Unwin, N. 1995 Acetylcholine receptor channel imaged in the open state. *Nature* **373**, 37–43.

Unwin, N. 1996 Projection structure of the nicotinic acetylcholine receptor: distinct conformations of the α-subunits. *J. Mol. Biol.* **257**, 586–596.

Unwin, N. 1998 The nicotinic acetylcholine receptor of the *Torpedo* electric ray. *J. Struct. Biol.* **121**, 181–190.

Unwin, P. N. T. & Ennis, P. D. 1983 Calcium-mediated changes in gap junction structure: evidence from the low angle X-ray pattern. *J. Cell Biol.* **97**, 1459–1466.

Unwin, P. N. T. & Ennis, P. D. 1984 Two configurations of a channel-forming membrane protein. *Nature* **307**, 609–613.

Unwin, P. N. T. & Henderson, R. 1975 Molecular structure determination by electron microscopy of unstained crystalline specimens. *J. Mol. Biol.* **94**, 425–440.

Unwin, P. N. T. & Zampighi, G. 1980 Structure of the junction between communicating cells. *Nature* **283**, 545–549.

Villarroel, A., Herlitze, S., Koenen, M. & Sakmann, B. 1991 Location of a threonine residue in the α-subunit M2 transmembrane segment that determines the ion flow through the acetylcholine receptor channel. *Proc. R. Soc. Lond.* B **243**, 69–74.

White, B. H. & Cohen, J. B. 1992 Agonist-induced changes in the structure of the acetylcholine receptor M2 regions revealed by photoincorporation of an uncharged nicotinic competitive antagonist. *J. Biol. Chem.* **267**, 15 770–15 783.

Whittaker, V. P. 1992 *The cholinergic neuron and its target*. Boston, MA: Birkhausser.

Williamson, P. T. F., Watts, J. A., Addona, G. H., Miller, K. W. & Watts, A. 2000 Dynamics and orientation of $N^{+}(CD_3)_3$-bromoacetylcholine bound to its binding site on the nicotinic acetylcholine receptor. *Proc. Natl Acad. Sci. USA*. (In the press.)

Wilson, G. G. & Karlin, A. 1998 The location of the gate in the acetylcholine receptor channel. *Neuron* **20**, 1269–1281.

Zenisek, D., Steyer, J. A. & Almers, W. 2000 Transport, capture and exocytosis of single synaptic vesicles at active zones. *Nature* **406**, 849–854.

PHILOSOPHICAL TRANSACTIONS OF THE ROYAL SOCIETY B BIOLOGICAL SCIENCES